Universiteit Leiden
The Netherlands

Protostellar jets and planet-forming disks: Witnessing the formation of Solar System analogues with interferometry
Tychoniec, Ł.

Cover Page

Universiteit Leiden

Leiden University
Repository

The handle http://hdl.handle.net/1887/3147349 holds various files of this Leiden University dissertation.

Author: Tychoniec, Ł.
Title: Protostellar jets and planet-forming disks: Witnessing the formation of Solar System analogues with interferometry
Issue date: 2021-03-09

1
Introduction

How did the Earth, Jupiter, the Sun, and the whole Solar System form? This basic curiosity has been a driver for philosophers, scientists, and astronomers for centuries. Limited to observations with the naked eye, ancient Greek philosophers commonly argued that the Earth was at the center of the Universe with the Sun and planets orbiting around her (e.g., Aristotle 370 B.C.; Ptolemei 120).

Copernicus (1543) and others refocused our perception of the Universe with the realization that the Earth is revolving around the Sun. With the progress in understanding of the laws of gravity, ideas about the beginnings of the Solar System were on the right track with the so-called "nebular hypothesis" (Swedenborg 1734; Kant 1755; Laplace 1796).

The emergence of modern astronomy with more and more powerful optical telescopes revealed stunning images of nebulosities across the sky, the most prominent catalogued in Messier catalog. Their nature – are they inside our Galaxy or are they galaxies on their own right – was famously debated by Harlow Shapley and Heber Curtis in 1920. The latter was proven right as the distance to the Andromeda galaxy by Opik (1922) was measured by observing its rotational movement. When Hubble (1929), measured distance to even more galaxies using the Cepheid method developed by Henrietta Leavitt, dimensions of the Universe were pushed almost to infinity. Not all of those nebulae are located millions of light years away. Some of the bright molecular clouds turned out to be located in our Galaxy, and identified as stellar nurseries, such as Orion Molecular Cloud. Those clouds are the primary spots to study the first stages of stars and planet formation. In the days of Hubble and Leavitt, however, the only evidence that planets can be formed around stars was our own Solar System.

End of twentieth century brought a new breakthrough, the discovery of planets around other stars. First planet was found around exotic pulsars (Wolszczan & Frail 1992), but soon after, planets orbiting much more familiar Sun-like stars were detected (Mayor & Queloz 1995). As of today, there are 4370 confirmed exoplanets detected (after exoplanet.eu database, as of 29th October 2020; Schneider et al. 2011). With those numerous detections it became clear that most planetary systems are very different from our own (Madhusudhan 2012; Winn & Fabrycky 2015); for example containing gas giants on a very close orbit, called hot Jupiters, or with many rocky planets closer to their star than Mercury is to the Sun. By pushing the limits of our understanding of the Universe, new questions arose: What is the origin of planetary systems and their diversity? How unique is the Solar System?

At the center of the question about the origin of our Solar System lies the understanding of the beginnings of stars and planets in general. Knowledge about star and planet forma-

tion is gained through astronomical observations of regions where star formation is currently ongoing, along with theoretical models and computational simulations that describe the process of making stars and planets. This thesis is an observational effort to characterize the early phases of star formation with a special focus on two crucial aspects of this process: **protostellar jets** and **embedded disks**. Special attention is paid to links between young protostars and the exoplanetary systems observed in the Milky Way. To understand the importance of jets and disk formation for the star formation process, a general overview of our current knowledge is provided.

1.1 Origin of solar-like stars

1.1.1 Collapse of a molecular cloud

Stars form in molecular clouds that consist predominantly of gas in which the main component by four orders of magnitude is molecular hydrogen (H_2). A small fraction of mass of such clouds (1%) is deposited in solid dust particles built out of refractory material, such as silicates and carbonaceous material; dust grains are often coated with ice mantles consisting of volatile material, such as water (H_2O), methanol (CH_3OH), and carbon monoxide (CO).

Molecular clouds are cold (10-20 K) and dense (10^3–10^6 particles per cm^3) and have ages up to tens of millions of years. Their relative youth compared with the age of the Milky Way has been one of the first arguments for the fact that the star formation is currently ongoing in our Galaxy (Ambartsumian 1947). Stars are predominantly formed in clustered environments (Lada & Lada 2003; Krumholz et al. 2014), however, those birthplaces can vary in terms of density and size (Ward-Thompson et al. 2007); large molecular clouds are observed to form dense filaments and fibers in which prestellar cores can form (André et al. 2010, 2014; Hacar et al. 2013; Tafalla & Hacar 2015). Many physical phenomena such as turbulence and magnetic fields are of importance at this stage (Goodman et al. 1998; McKee & Ostriker 2007).

Eventually cores begin to collapse under their own gravity. Such a core needs to be cold and dense enough for the collapse to satisfy the Jeans criterion (Jeans 1928). On cloud scale, star formation is not a very efficient process, with between 2–4% of gas and dust converted into stars; on the other hand, prestellar cores have up to 30% of star formation efficiency (Alves et al. 2007; Evans et al. 2009; Offner & Arce 2014).

Collapsing clouds form central dense cores, which become optically thick. As pressure and temperature rise, the accretion is halted. Such a core is called a First Hydrostatic Stellar Core (FHSC), it heats up until it reaches the temperature needed to dissociate molecular hydrogen; this process causes the imbalance of equilibrium allowing it to collapse further – a protostar is born (Larson 1969).

Models and evolutionary schemes of star formation are simplified in a sense that they often describe an isolated, single star in the making. However, it should be noted that around 50% of mature solar-mass stars are found in multiple systems (Raghavan et al. 2010), and the multiplicity fraction is even larger in the early stages (Tobin et al. 2016).

Table 1.1: Observational markers of protostellar evolution

Class	α_{IR}	$L_{\mathrm{submm}}/L_{\mathrm{bol}}$	T_{bol} [K]
0	-	$\geq 0.5\%$	≤ 70
I	≥ 0.3	$< 0.5\%$	$70 - 650$
Flat	$0.3 - $-0.3	–	–
II	$-0.3 - $-1.6	–	$650 - 2800$
III	$\leq $-1.6	–	≥ 2800

1.1.2 Protostellar classification

Low-mass protostars are divided into phenomenological *Classes*, which employ different observational characteristics of young stars and their surroundings. The infrared spectral index

$$\alpha_{\mathrm{IR}} = \frac{d \, \log \lambda F_\lambda}{d \, \log \lambda},\tag{1.1}$$

with λ between 2 and 20 μm, has been the first method of defining the evolutionary stage of a protostar, with redder sources (i.e. brighter emission at longer wavelengths and positive α_{IR}) corresponding to younger evolutionary stages (Lada & Wilking 1984). The bolometric temperature associated with the protostellar spectral energy distribution (SED) is the temperature of a blackbody having the same mean frequency. This temperature is an alternative method to classify protostars in different observational classes (Myers & Ladd 1993; Chen et al. 1995). Following the discovery of even redder, Class 0 protostars (André et al. 1993), the submillimeter luminosity as a fraction of total luminosity has been introduced as another border between Class 0 and Class I. Fig. 1.1 presents the overview of protostellar classes along with typical SED for each of them (summarized in Tab. 5.1).
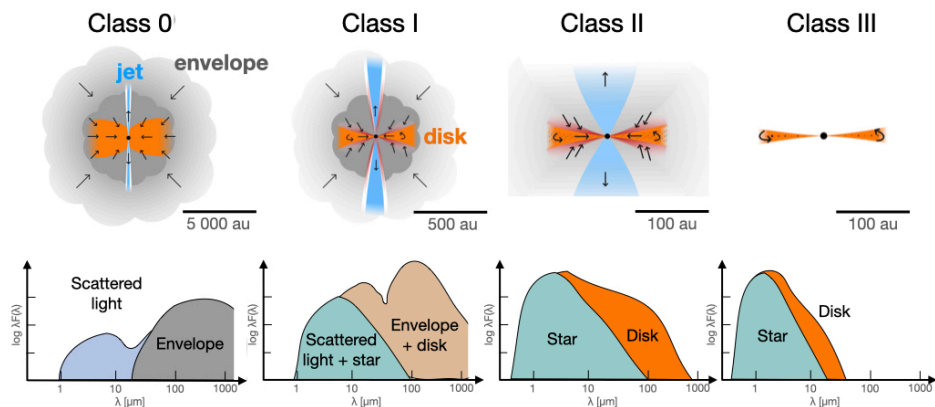

Figure 1.1: *Top*: Schematic view of the protostellar systems at different stages of evolution. *Bottom*: Sketch of mid-infrared SED protostellar classes. Adapted from figure by M. Persson.

Class 0 protostellar systems are deeply embedded in their parent cloud and most of the mass is residing in this natal envelope. Accretion rates are at their highest in this stage and the molecular jet and outflow are most prominent. Due to the conservation of angular momentum, disks already form in this stage (Tobin et al. 2012; Murillo et al. 2013; Maury

et al. 2019), although it is often difficult to disentangle them from a surrounding envelope. Measurements of disk masses in the Class 0 phase show that their disks typically contain 1–10% of the mass of the envelope. These sources are also associated with the richest molecular complexity, as high temperatures of the inner regions of Class 0 systems allow for thermal desorption of ices in so-called hot cores (Herbst & van Dishoeck 2009).

Class I systems are physically characterized as sources with most of their masses already transferred from the envelope to the disk and protostar. Outflows are much weaker and usually they have much wider opening angles compared with Class 0 sources (Arce & Sargent 2006). Less chemical complexity is seen as the gas temperature decreases, except for cases of outbursting sources (van 't Hoff et al. 2018c; Lee et al. 2019b). Disks are clearly observed at this stage with masses between 20–60% of the envelope; this value reaches 70–98% in disks with confirmed Keplerian rotation (Jørgensen et al. 2009). First examples of rings and gaps in those disks can be observed (ALMA Partnership et al. 2015; Segura-Cox et al. 2020; Sheehan & Eisner 2017, 2018; Sheehan et al. 2020), suggesting that planet formation can already start at this early stage. Flat Spectrum sources are sometimes also designated as a transition between Class I and Class II (Greene et al. 1994).

Class II systems are characterized by optically visible pre-main sequence stars, which already begin fusion of deuterium and show rich atomic line emission spectra at visible and near-IR light. These sources are often called T-Tauri stars, named after the prototypical object of this group. In Class II systems, disks can be clearly observed at submillimeter wavelengths (Williams & Cieza 2011), often with rings and gaps (Andrews et al. 2018; Huang et al. 2018), that can be signs of ongoing planet formation. Typical Class II disks are an order of magnitude less massive than Class 0/I disks (Tychoniec et al. 2018b).

Class III systems have only residual emission from a disk as most of their dust is either accreted or assembled in planetesimals and planets. Continuing contraction of the pre-main sequence star causes its temperature to rise high enough so that hydrogen fusion can commence and the star becomes a main sequence star.

Protostellar *Stages* describe the physical properties of the system, resulting from the interpretation and modeling of the observational properties of evolutionary classes. The properties inferred from observations can be the relative masses of the protostar, disk and envelope, or the accretion rate onto the protostar (e.g., van Kempen et al. 2009b). In Stage 0 the mass of the system is dominated by the envelope, while in Stage I, the most mass is already accumulated in the disk and the protostar. Stage II is characterized by decreased accretion rates compared with the previous ones, and the almost negligible mass of the envelope. In Stage III the disk almost disappears and consists mostly of dust, and the accretion stops (Shu et al. 1987; Whitney et al. 2003; Robitaille et al. 2006). The distinction between Stages and Classes is made as some observational properties can be altered by environment, for example, extincted or edge-on Stage II sources can masquerade as Class I systems or Flat Spectrum sources (van Kempen et al. 2009b; Crapsi et al. 2008; Hatchell et al. 2007).

1.1.3   Observations of protostars

From the described properties of Class 0 and I protostars it is clear that studies of the youngest systems are challenging. Low temperatures and high extinctions mean that the bulk of the emission occurs at mid-infrared and longer wavelengths (Fig. 1.1).

Most infrared wavelengths are efficiently blocked by the Earth's atmosphere. That is why progress in infrared astronomy requires space-borne telescopes. ISO and *Spitzer*, among other facilities, revealed the importance of infrared observations of protostars, especially for

their classification and studying the ice content of protostellar envelopes and disks (Boogert et al. 2008). The *Herschel Space Obseratory*, with its large 3.5m dish, revolutionized our view of protostars in the far-IR, by observing water in star-forming regions (van Dishoeck et al. 2011; Hogerheijde et al. 2011); quantifying the heating and cooling mechanisms in protostars (van Kempen et al. 2010; Kristensen et al. 2012; Green et al. 2013; Karska et al. 2018) and mapping molecular clouds with dust continuum emission (André et al. 2014).

Astronomical observations at radio wavelengths are possible from the ground, however, at very dry conditions. Additionally to achieve high angular resolution, interferometry needs to be employed to combine the signal from multiple radio dishes to achieve a spatial resolution competing with optical telescopes. Early studies with single-dish telescopes, before interferometry became available, provided a wealth of information about the star-formation process on scales of 0.05 pc. They revealed the stunning chemical complexity of young protostars, such as IRAS 16293-2422 (van Dishoeck et al. 1995). Single-dish studies are especially useful in probing envelope and cloud-scale emission (e.g., Blake et al. 1994; Jørgensen et al. 2002; Maret et al. 2005; Murillo et al. 2018). The advent of interferometric observations that boost the spatial resolution and collecting power of the submillimeter observations, with facilities such as OVRO, BIMA/CARMA, SMA, and IRAM-PdBI, allowed the protostellar systems to be resolved at this crucial part of spectra, where most of the action happens for the young protostars,

The big leap forward in studying star formation on Solar System scales was made possible by the Atacama Large Millimeter/submillimeter Array (ALMA) on the Chajnantor Plateau in Chile. It has fantastic conditions to observe millimeter universe, at 5000 meters above the sea level, at one of the driest places on Earth. ALMA has been able to resolve the thermal emission from cold dust in protoplanetary disks providing stunning images (van der Marel et al. 2013; ALMA Partnership et al. 2015; Andrews et al. 2018). Its remarkable sensitivity also allowed for unprecedented studies of chemical complexity associated with protostars (Jørgensen et al. 2016). The Very Large Array (VLA) in New Mexico, USA, provides insight into longer wavelengths at subarcsecond resolution. Centimeter wavelengths are a window to observe different physical processes such as ionized and synchrotron emission from young stars. This thesis utilizes the capabilities of ALMA and VLA to probe young Class 0 and Class I protostars. It also aims to pave the way with interferometric observations to new frontiers of studies of star-forming regions that will be made available by the *James Webb Space Telescope* (JWST), set to launch in late 2021.

1.2   Molecules as tracers of protostellar systems

Rotational transitions of molecules allows the protostellar system to be dissected into physical components. Molecular tracers are also a powerful tool to probe densities, temperatures, UV fields, chemical abundances and kinematics (e.g., van Dishoeck & Blake 1998; van Dishoeck & Hogerheijde 1999; Evans 1999). The different components of protostellar systems vary significantly in their physical conditions. We divide the protostellar system into its key components that are illustrated in Fig. 5.1.

Envelope. The envelope surrounding a protostar contains the material that fuels in the accretion process onto the star and disk. The physical conditions in the outer envelope on scales of a few 1000 au are reminiscent of those of starless cores, and their chemical composition is directly inherited from the cloud out of which the star is being born (Caselli & Ceccarelli 2012). Systematic motions such as infall or expansion can occur but otherwise they have low turbulence and narrow line profiles indicative of quiescent gas. Observations
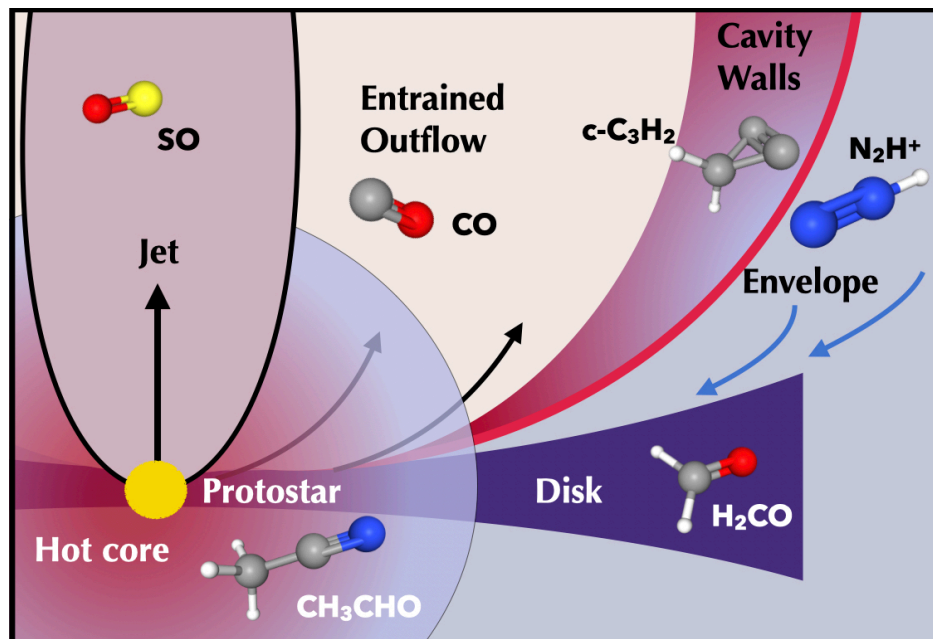
Figure 1.2: Cartoon illustrating the physical components of a protostellar system. Arrows indicate the direction of material in motion; the protostellar jet emerges from the innermost region of the system, but not exclusively from the protostar itself. The size of the envelope with respect to the disk can vary depending on the disk size and temperature profile of the system. Example molecule used is showed in frame, which color correspond to a respective physical component that the molecule is tracing. Molecule images from: https://pubchem.ncbi.nlm.nih.gov/.

with interferometers are challenging because most of the envelope material is resolved out at subarcsecond resolution. Single-dish studies have been very useful in probing the entirety of the envelope emission and pointing to the importance of molecular tracers and line ratios in understanding the physics on large scales (e.g., Blake et al. 1994; van Dishoeck et al. 1995; Ceccarelli et al. 2000; Jørgensen et al. 2002; Maret et al. 2004; Jørgensen et al. 2004b; Emprechtinger et al. 2009; Tobin et al. 2013; Carney et al. 2016; Murillo et al. 2018). Interferometric observations showed a complex geometry of the envelope, and revealed the chemical sensitivity to its temperature profile (Jørgensen et al. 2004a; Tobin et al. 2011). The envelope can be probed by cold and dense gas tracers such as CO isotopologues ^{13}CO and C^{18}O, or ions like N$_2$H$^+$, H^{13}CO$^+$ and their deuterated counterparts N$_2$D$^+$ and DCO$^+$ (e.g., Chen et al. 2007; Tobin et al. 2013; van 't Hoff et al. 2018a; Hsieh et al. 2019b). Deuterium fractionation is especially enhanced in cold environments (Caselli et al. 1999).

Outflows. As the material is accreting from the envelope onto the disk and protostar, excess angular momentum is released by means of collimated high-velocity jets which originate from the innermost star-disk interface regions of the protostellar system. In the earliest stages when the mass loss is at its peak, the densities are high enough to form molecules in the internal shocks in the jet (Bachiller & Gomez-Gonzalez 1992; Tafalla et al. 2010). Jets consist initially of mostly molecular material, but undergo significant chemical evolution along

the protostellar lifetime (Nisini et al. 2015). In the molecular stage of the jet, molecules that are enhanced by grain-destruction such as SiO and SO can be observed (Tafalla et al. 2010; Tychoniec et al. 2019; Tabone et al. 2020; Lee 2020).

Much slower (<20 km s^{-1}) and less collimated gas moving away from the protostar is called an outflow. It consists mostly of envelope material, and CO as the most abundant molecule after H$_2$ is abundantly seen in the entrained gas and wide-angle wind launched from the disk (e.g., Arce & Sargent 2006; Plunkett et al. 2013; Bjerkeli et al. 2016). Temperatures in shocks are much higher than in the surrounding envelope, up to a few thousand K, and sputtering of grain cores and ice mantles can further result in unique chemical signatures from molecules like CH$_3$OH, C$_2$H$_5$OH, CH$_3$CHO (e.g., Arce et al. 2008; Rodríguez et al. 2017; Lefloch et al. 2017; Codella et al. 2020).

Outflow cavity walls. These are the narrow zones in between the cold dense quiescent envelope material and the lower-density warm cone where outflows are propagating at large velocities. Cavity walls are exposed to UV radiation from the accreting star-disk boundary layer, which can escape through the outflow cavity without being extincted (Spaans et al. 1995). This creates conditions similar to those found in Photon Dominated Regions (PDRs), which occur throughout the interstellar medium near sources of intense UV radiation (Hollenbach & Tielens 1997). In units of the interstellar radiation field (ISRF, Draine 1978), typical values of 10^2-10^3 are found on scales of ∼ 1000 au (van Kempen et al. 2009a; Yıldız et al. 2012; Benz et al. 2016; Karska et al. 2018), which is comparable to Horsehead Nebula PDR region (Abergel et al. 2003), while in more energetic regions such as Orion nebula the radiation field exceeds 10^4 times the interstellar value (Marconi et al. 1998). C$_2$H and c-C$_3$H$_2$ are observed in this layer, likely formed from abundant carbon atoms, dissociated out of CO molecules by the UV (Jørgensen et al. 2013; Oya et al. 2017)

Young disk. In the inner envelope, a protoplanetary disk starts to form as the natural outcome of a rotating collapsing core (Cassen & Moosman 1981; Terebey et al. 1984). At early stages it is difficult to identify kinematically whether the so-called embedded disk is rotationally-supported, since any molecular emission from the disk is readily overwhelmed by that from the envelope. In recent years several embedded disks have been identified to have Keplerian rotational structure on scales of ∼100 au with tracers such as H$_2$CO and C^{18}O (Tobin et al. 2012; Murillo et al. 2013; Codella et al. 2014; Yen et al. 2017). Molecular tracers in young disks, apart from providing the kinematic information, can probe their temperature structure as well (van 't Hoff et al. 2018b). Hydrodynamical models of disk formation also predict an accretion shock as envelope material falls onto the disk (Neufeld & Hollenbach 1994; Li et al. 2011). Some molecules, notably SO and SO$_2$, are proposed as tracers of such shocks (Yen et al. 2014; Sakai et al. 2014b, 2017; Artur de la Villarmois et al. 2019).

Hot core. In the innermost part of the envelope on scales of the disk, temperatures rise above 100 K, so any water and complex organic molecules (COMs) contained in ices are released from the grains back into the gas where they are readily observed at submillimeter wavelengths. This region with its unique chemical richness is called the hot core, or to distinguish it from its high-mass counterpart, hot corino (Herbst & van Dishoeck 2009). High signal-to-noise and high resolution spectra, especially with ALMA and IRAM-PdBI of low-mass protostars revealed that inner envelopes of young protostars are chemically rich, showing prominent emission from e.g., CH$_3$CHO, CH$_3$OCHO (e.g., Sakai et al. 2014a; Jørgensen et al. 2016; López-Sepulcre et al. 2017; Codella et al. 2018; Manigand et al. 2020; van Gelder et al. 2020; Bianchi et al. 2020).
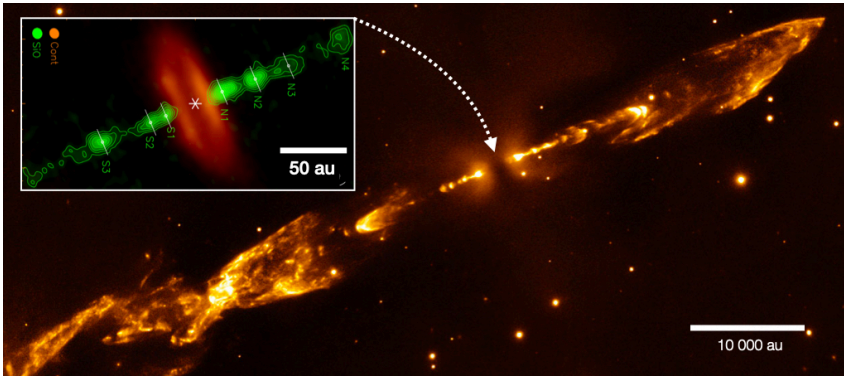
Figure 1.3: Image of the protostellar outflow toward HH212 protostar, through 2.12 μm shocked H$_2$ observations with VLT (McCaughrean 1994). Inset shows the molecular jet seen in SiO 5–4 transition at 1.3 mm and the continuum emission from the disk at 1.3 mm (Lee et al. 2017).

1.3   Protostellar jets and outflows

Outflows from protostars are a staggering emanation of stars being born. They were first observed in optical light as Herbig-Haro objects rich in spectral lines (Herbig 1950); then with the emergence of radio astronomy, observations of CO line profiles revealed that velocities of these objects are consistent with outflowing, entrained gas from protostars (Snell et al. 1980). Ever since our understanding of their importance to the star formation process has been increasing. Jets and winds from protostars are invoked to release excess angular momentum from the star plus disk system, allowing the accretion to continue (Ferreira et al. 2006). Substantial amounts of material from the envelope are removed from the system by means of outflows. Fig. 1.3 shows the outflow from the HH212-mm protostar in the mid-IR, which traces the shocks with the envelope material. In the submillimeter wavelengths the jet directly launched from the innermost regions can be observed with molecular tracers.

1.3.1   Jet launching and observations

The mechanism of the outflow launching process is still debated. The general consensus is that magnetohydrodynamical (MHD) winds are launched from the innermost regions of the system: either from the protostar-disk interface (X-wind; Shu et al. 1994, 2000) or at larger radii of the disk (disk wind; Pudritz & Norman 1983; Ferreira 1997). This jet entrains the envelope material that can be observed as the low-velocity molecular outflow (Raga et al. 1993).

The launching of the jet is strongly linked to the accretion process. These jets are expected to consist of material directly released from the launching regions, as opposed to the low-velocity outflows which consist mostly of entrained material.

The jet component is observed primarily as so-called *bullets* of concentrated emission, in often symmetric separations, ejected from the central source at high velocities (Guilloteau et al. 1992; Bachiller et al. 1994; Santiago-García et al. 2009; Hirano et al. 2010; Plunkett et al. 2015). Resolved high-velocity bullets show a kinematic structure that is consistent with sideways ejection (Tafalla et al. 2017). The systematically displaced bullets of material
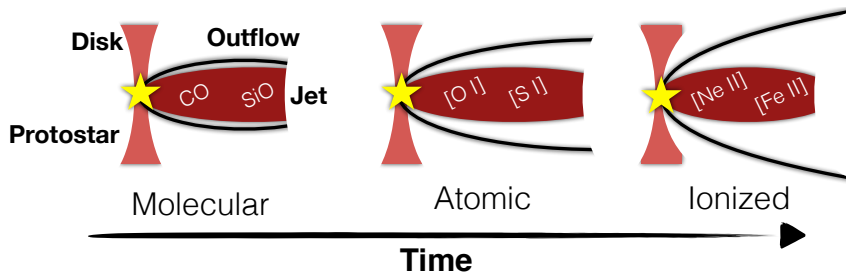
Figure 1.4: Cartoon presenting the chemical evolution of the jet based on the scheme described by Nisini et al. (2015). Young Class 0 jet is mostly molecular, with high mass-loss rates creating conditions for molecule formation; as the mass-loss rate decreases, so does the density in the jet, and photodissociation results in more atomic material; in the late stages the ionized component becomes more prominent.

are explained by the variability of an accretion process. Thus, jets are proposed to provide a record of past episodic accretion events (Raga et al. 1993; Lee 2020).

The jet composition is observed to evolve from mostly molecular, through atomic to ionized material (Nisini et al. 2015). Fig. 1.4 illustrates this process. This evolution is attributed to the change in physical conditions in the jet: lower mass flux results in lower density of material on the way, making the formation of molecules in the bullet less favorable. Moreover, the bullets can be efficiently penetrated by the energetic radiation from the protostar.

1.3.2 Entrained outflow

Surrounding the high-velocity jet is a low-velocity outflow, which consists mostly of entrained envelope material. The properties of outflows are strongly dependent on the evolutionary stage. There is an observed link between the bolometric luminosity of the protostar and its outflow force (Cabrit & Bertout 1992; Bontemps et al. 1996; Mottram et al. 2017). Probing outflows at the earliest stages, when they are most prominent, offers best insight into their properties and interactions with the surrounding envelope.

Shocks, violent encounters between the supersonic jet and outflow with the ambient material, are an important manifestation of the star formation process. Shocks can reveal rich chemistry as high-temperatures created in the shocked regions can lead to formation of some key molecules such as H_2O (Draine et al. 1983; Neufeld & Kaufman 1993; Herczeg et al. 2012; Karska et al. 2014a). Mechanical interactions between the outflows and the envelope can result in sputtering of the ices from the grain, revealing their composition (Arce et al. 2008).

1.3.3 Radio jets

Highly ionized material in shocks can produce thermal emission at radio wavelengths, which is characterized by spectral index $\alpha > -0.1$, where $F_\nu \sim \nu^\alpha$. Free-free emission (*bremsstrahlung*) is produced in ionized medium where free electrons are slowed down, releasing photons at radio wavelengths with typical spectral index of $\alpha = 0.5$. The most important evidence for the link between free-free emission and jets is that the free-free luminosity is related to the outflow force (Cabrit & Bertout 1992) and that, if resolved, such radio emission is observed to

be elongated along the outflow direction (Rodríguez & Reipurth 1989; Anglada et al. 1996; Tychoniec et al. 2018c). It is important to highlight that for studying dust continuum at longer wavelengths, free-free emission can contribute to this flux, which needs to be corrected for.

In a handful of protostars the radio emission shows negative spectral indices $\alpha < -0.1$. at >4 cm wavelengths which is a sign of non-thermal emission (Ainsworth et al. 2014; Tychoniec et al. 2018c). It originates from gyrosynchrotron radiation. Such a mechanism can occur even in low-velocity shocks, where protons may be accelerated to relativistic velocities (Padovani et al. 2016). This process can be relevant as a source of cosmic rays in protostellar envelopes which are otherwise attenuated (Padovani et al. 2013).

1.4 From embedded to planet-hosting disks

Disks of gas and dust surrounding protostars play a central role in understanding the origin of planets as their birthplaces (e.g., Lissauer 1993). The chemical composition of planets depends on that of the disk (Öberg et al. 2011; Madhusudhan 2019) and the physical conditions in the disks are of crucial importance to the mechanism of planet formation.

1.4.1 Formation of an embedded disk

Disk formation starts in the early stages of the star formation, when due to the conservation of the angular momentum, a flattened, rotating structure is created around a protostar (Cassen & Moosman 1981; Terebey et al. 1984). The disk plays a central role in transport of the material from the envelope to the protostar. Observations show that disks are formed rapidly and that the bulk of the mass reservoir is accreted early onto the disk from the envelope, within a few 10^5 yrs after the cloud collapse (Hueso & Guillot 2005; Jørgensen et al. 2009; Williams & Cieza 2011). The observed compact continuum flux due to the dust emission decreases with time, with dust either accreted onto the star or grown into larger bodies that are not detected at submillimeter wavelengths.

Disks surrounding a Class 0/I protostars are called the *embedded disks* as they are still deeply covered in their natal envelope. As protostar enters pre-main sequence (Class II onwards), a well-defined disk around it is called a *protoplanetary disks*, however, emerging paradigm of early planet formation suggest that a name *planet-hosting* disk is more accurate.

Early theoretical models of disk formation suggested that magnetic fields would inhibit the formation of the embedded disks larger than 10 au, due to magnetic braking (Mellon & Li 2008). While majority of embedded disks are indeed small (< 50 au dust size), protostellar disks are now routinely observed (Tobin et al. 2012; Murillo et al. 2013; Segura-Cox et al. 2016; Maury et al. 2019; Tobin et al. 2020), and the magnetic braking might not be as problematic to disk formation as previously thought.

Single-dish observations show that there are large grains in young disks (Weintraub et al. 1989), but only with interferometric studies can resolved disk images at millimeter wavelengths be observed. Early observations with first radio interferometers such as BIMA, OVRO/CARMA, Nobeyama Array, IRAM-PdBI and SMA offered moderate resolution observations of protostellar envelopes, and only with visibility analysis it became possible to distinguish embedded disk from the envelope and show evidence for grain growth (Kawabe et al. 1993; Looney et al. 2000; Jørgensen et al. 2004a, 2009; Kwon et al. 2015).

The interplay of the solid and gas content of disks is fundamental for disk evolution and planet formation. Large grains are drifting inwards due to the drag they experience from the surrounding gas. Young disks are warm, which means that molecular species such as CO

are present in the gas phase even out to large radii (Harsono et al. 2015a; van 't Hoff et al. 2018a, 2020). As the disk cools down, molecules settle onto the grains at the distance from the protostar where the freeze-out temperature of a molecule is reached, at their *iceline*. This results in molecular depletion in the gas phase. As the ice composition of grains changes, their physical properties are altered too, especially freeze-out of H_2O enhances grain growth by coagulation (Stevenson & Lunine 1988). The composition of planetary atmospheres is largely dependent on the location of planetary embryos with respect to the icelines (Öberg et al. 2011; Cridland et al. 2019; Eistrup et al. 2018; Notsu et al. 2020).

However, before we can start discussing factors that determine the composition of atmospheres and cores of planets, there needs to be enough material to produce planets in the first place. Due to the depletion and optical thickness of gas, dust is the most common mass tracer in the disks. This thesis is concerned with dust masses of embedded disks. It is without doubt that gas also plays a crucial role and future observations at high-resolution and sensitivity with ALMA will allow to further constrain also the gas masses.
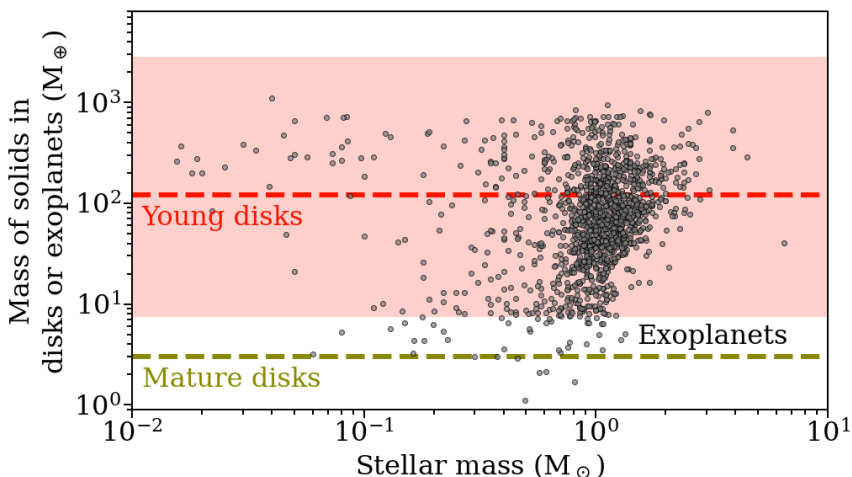

Figure 1.5: Plot showing the distribution of masses of exoplanetary systems obtained from the exoplanet.eu catalog (Schneider et al. 2011), for the planets around main sequence stars with the measured masses. Shaded areas mark the range of the best estimation of the dust disk masses in Perseus from (Tychoniec et al. 2020) young disks (Class 0 and Class I) calculated from the VLA fluxes. Median is indicated with dashed line. The median mass of the Class II disks in Lupus, 3 $M_\oplus$ (Ansdell et al. 2016) is showed in yellow. The masses of the solids in exoplanetary systems are plotted against the stellar mass of the host star.

1.4.2 Determination of embedded disk masses

Submillimeter continuum observations of protostellar systems at high-resolution can be utilized to calculate the dust mass of disks following the equation from Hildebrand (1983):

$$M = \frac{D^2 F_\nu}{\kappa_\nu B_\nu(T_{\text{dust}})},$$ (1.2)

with D as the distance to the source, B_ν the Planck function for a temperature T_{dust}, and κ_ν the dust opacity (dust mass absorption coefficient) with the assumption of optically thin

emission. Typically the dust temperature is assumed to be 30 K for young disks, similar to protostellar envelopes (Whitney et al. 2003), while more evolved Class II disks are presumably colder at 20 K (Andrews & Williams 2005).

The classic value for κ_ν is based on the Ossenkopf & Henning (1994) calculation $\kappa_{1.3mm} = 0.9 \text{ cm}^2 \text{ g}^{-1}$. The dust opacity is a major source of uncertainty in the dust mass estimation. Panić et al. (2008) summarize a range of literature values between 0.1 and 2 cm^2 g^{-1} at 1.3 mm. Higher values are possible if grains have more amorphous carbon than typically assumed (Birnstiel et al. 2018).

The spectral index at millimeter wavelengths α ($F_\nu \sim \nu^\alpha$) can be used to estimate the grain size distribution. The dust emissivity index $\beta = 2 - \alpha$ is defined to indicate the dependence of the dust opacity on frequency ($\kappa_\nu \sim \nu^\beta$). In the interstellar medium the value of β is estimated to be ~1.8 (Draine 2006). In the optically thin limit, a low value of β can point to dust growth (e.g., Natta & Testi 2004; Ricci et al. 2010; Testi et al. 2014).

Masses of embedded disks are difficult to measure, as the envelope is still bright during early stages of evolution. With interferometric observations the envelope is resolved out and the disk can be directly observed. However, the dust tends to be optically thick at submillimeter wavelengths. VLA Ka-band data (9 mm) promise to overcome those limitations, by being sensitive only to larger grains in the densest part of the embedded disk and being optically thin. The major limitation of Ka-band observations is the contamination from free-free emission at those wavelengths.

1.5   Formation of planets

Planets materialize in disks of gas and dust surrounding young stars. Surveys of mature protoplanetary (planet-hosting) disks enabled by ALMA show that their masses are low; in fact so low that formation of currently observed exoplanetary systems would not be possible from the available reservoir of dust (Ansdell et al. 2017; Manara et al. 2018). ALMA and VLA synergy enabled surveys of embedded disks showing that their masses are 5 to 10 times larger than in Class II sources. (Tychoniec et al. 2018c; Tobin et al. 2020). Tychoniec et al. (2020) show that if planet formation starts early, in Class 0/I disks, the dust reservoir is sufficient (Fig. 1.5). Here we present a brief overview of the current concepts on how planets are formed.

The two leading models of the formation of planets are *core accretion* (Mizuno 1980; Pollack et al. 1996) and *gravitational instability* (Kuiper 1951; Cameron 1978; Boss 1997). In the core accretion scenario, dust is first accumulated into larger bodies (planetesimals), through, for example, the streaming instability (Youdin & Goodman 2005). Those planetesimals can attract more and more dust. Models distinguish *pebble accretion*, where parent planetesimal accretes small dust grains, called pebbles (Ormel & Klahr 2010; Lambrechts & Johansen 2012; Johansen & Lambrechts 2017) and *planetesimal accretion* where planetesimals grow through collisions with each other (Mousis et al. 2009). Regardless of the formation route, if a core grows to the size of 10 M$_\oplus$, it can accrete gas to form a gas giant.

Both planetesimal and pebble accretion have their shortcomings. Planetesimal accretion appears to take too much time, and by the time the core could grow to the size it attracts the gas, there is not much gas left in the disk (Goldreich et al. 2004). On the other hand, planetesimal accretion is very efficient, and eventually most of the planetesimals could be merged into planets (Alibert et al. 2013). Pebble accretion is very fast but not efficient with a maximum efficiency of converting dust disk mass to planets of 10% (Ormel 2017), or up to 30% if multiple planets are produced (Bitsch et al. 2019). This means that while planets can

form early, massive disks are required to produce massive systems. Also there is the need for a large planetesimal that would accrete pebbles needs to start with.

In the gravitational instability scenario, a massive disk becomes gravitationally unstable quickly and collapses with gas and dust to form a giant planet. The main problem with this formation route is the prediction of comparable chemical composition between a planet and a host star which is typically not observed (Thorngren et al. 2016). Another question is whether disks can become unstable.

Both core accretion and gravitational instability scenarios have limitations and the problem of planet formation is far from being solved. Large eccentricities and close orbits observed toward exoplanetary systems are difficult to reproduce with either models, however, this is usually explained by the post-formation dynamical evolution of the systems (Winn & Fabrycky 2015; Dawson & Johnson 2018).

An important input parameter for models of planet formation is the mass reservoir available for the process. This is strongly dependent on the timescale of planet formation. In this thesis, strong evidence is provided that planet formation starts early (Tychoniec et al. 2020). There are several other premises of early planet formation: (i) distribution of populations of meteorites in Solar System (Kruijer et al. 2014), (ii) observed rapid grain growth in Class 0/I (Harsono et al. 2018), (iii) deficiency of masses in mature disks (Williams 2012; Ansdell et al. 2017), (iv) substructures in Class I disks (Sheehan et al. 2020; Segura-Cox et al. 2020).

1.6   This thesis

This thesis presents observational insight into the earliest stages of star and planet formation. With the aid of the ALMA and VLA interferometers, protostellar jets and disks are characterized, setting the stage for future JWST–MIRI observations. The content of the thesis is as follows:

Chapter 2 presents results from the VLA Nascent Disk and Multiplicity Survey (VANDAM) of all Class 0/I protostars in the Perseus molecular cloud, with 4.1 and 6.4 cm (C-band) observations. Toward a hundred protostars we investigated the correlation between free-free emission and protostellar properties, showing a significant dependence of free-free emission on stellar properties. We also found that free-free emission is weakly correlated with J-type shock tracers. A very important outcome of this study was to use our measurements of the free-free component to correct the flux at 9 mm. With this correction we were able to compare the Class 0/I disk masses with those Class II systems for an unbiased sample for the first time. This provided important clues that there is much more dust available for planet formation at the early stages of star formation.

Chapter 3 is the continuation of the work from Chapter 2. We collected ALMA observations of all embedded disks in Perseus, to compare with VLA measurements. Using measurements between 1 and 9 mm we derive an average spectral index α = 2.5, showing that significant grain growth occurs in the early stages. We also compare the revised masses of embedded disks with the masses of available exoplanets to find that dust masses of Class 0/I sources in Perseus are sufficient to explain the solid content of the currently observed population of gas giants with efficiency of 10–30%. We also point out that most massive exoplanetary systems might require a higher efficiency of planet formation than single-planet systems.

Chapter 4 presents ALMA observations of high-velocity molecular jets in Serpens. The high detection rate of those jets suggests that they are likely more common than previously thought. The chemical differentiation between the low and high-velocity gas proves the

different physical origin of the two: the former being entrained material and the latter being the gas directly launched from the inner regions of the star-disk system. Our data indicate that the C/O ratio in the EHV gas is lower than in the entrained outflow. A detection of H_2CO in one of the molecular bullets tentatively suggests that dust is launched with the jet.

Chapter 5 is an effort to pinpoint chemical tracers to the physical components of the young protostellar systems at the Solar System scales (50 au) . Cold gas tracers like $C^{18}O$, DCO^+ and N_2D^+, associated with the freeze-out of CO are tracing quiescent envelope material. Shock tracers such as SiO and SO are seen in the outflow; additionally ice-mantle products released with the shock are also detected. SiO, SO and occasionally H_2CO are detected in the high-velocity molecular jet. The cavity walls show tracers of UV-irradiation such as hydrocarbons C_2H and $c\text{-}C_3H_2$ as well as CN. The hot inner envelope, apart from complex organic molecules (COMs), also presents compact emission from small molecules like H_2S, SO, OCS and $H^{13}CN$, most likely related to thermal ice sublimation or accretion shocks.

This thesis can be summarized as follows: Planet formation must start early (< 0.5 Myr), Class 0 and Class I protostars are massive enough to make planets. Therefore characterization of young protostars is essential. Protostellar jets are an important component of the star formation process, it seems that molecular jets are ubiquitous and they may allow to study the composition of the inner regions directly.

The main conclusions of this thesis are:

- Free-free emission from protostars is well correlated with bolometric luminosity and outflow force. The nature of radio emission does not evolve from Class 0 to Class I

- Embedded Class 0 and I disks are more massive than Class II disks, by an order of magnitude. Class 0 disk masses are larger than Class I by a factor of 3, if the same dust temperature is assumed, which suggests that the disk mass is set rapidly.

- Planet formation must start already in the Class 0 systems at ∼ 0.1 Myr in order to explain the solid content of currently observed exoplanets.

- Extremely high-velocity jets are more ubiquitous in young protostars than previously thought.

- Molecular tracers observed with interferometers are a powerful tool to discern the physical components of the protostellar systems.

The future is bright for interferometric observations of protostars. With ALMA in full swing we expect many high-resolution observations of young disks, revealing structures showing signs of planet formation in earliest stages. Multi-wavelengths studies of disks will be able to probe the properties of dust in those disks. Observations of molecular jets with many transitions of molecules will enable characterization of physical conditions and will be able to provide constraints on the atomic abundances of the gas launched with the jet and its dust content.

The unique spectral coverage of JWST-MIRI instrument at 5-28 μm, virtually unreachable from the ground, will unveil the ice composition of the protostellar systems. Simultaneously, the gas content will be mapped with the MIRI IFU unit at up to 0.2" resolution. Figure 1.6 illustrates the synergy between ALMA and JWST on the example of one of the guaranteed targets for Cycle 1 JWST observations. Information on the high temperature processes in
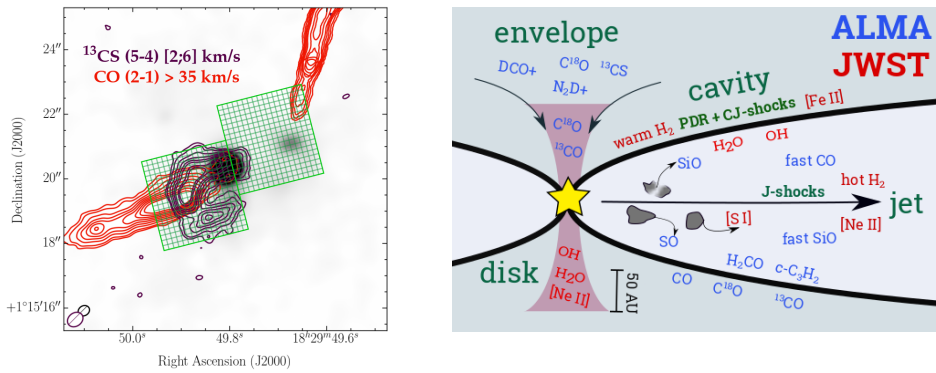
Figure 1.6: *Left:* Serpens SMM1 protostellar system, one of the guaranteed time targets for the JWST/MIRI observations. Map shows ALMA observations from Hull et al. (2016) of dense gas tracer ^{13}CS in purple and the molecular jet mapped by high-velocity CO emission in red contours. 1.3 mm continuum shown in grayscale. Overlaid in green is the MIRI-MRS footprint at its highest resolution which will provide R~3000 spectra from each of the IFU pixels at maximum resolution of 0.2″. *Right:* Cartoon image of the various emission components observable with ALMA (in blue) and with JWST/MIRI (red). ALMA probes the molecular part of the jet and entrained outflow material, and delineates the disk and envelope. The mid-IR lines are diagnostics of the hot currently shocked gas but their emission has so far been spatially unresolved. The combination of ALMA and JWST/MIRI will be able to resolve the physical components for the first time.

young stars coupled with ALMA observations of colder molecular gas with kinematic information are going to revolutionize the field of star and planet formation on Solar System scales and inspire new generations of astronomers.